THE JOURNAL OF PHYSICAL CHEMISTRY B

Article

pubs.acs.org/JPCB

Electrical Coupling in Ensembles of Nonexcitable Cells: Modeling the Spatial Map of Single Cell Potentials

Javier Cervera,* Jose Antonio Manzanares, and Salvador Mafe*

Departament de Termodinàmica, Universitat de València, E-46100 Burjassot, Spain

Supporting Information

ABSTRACT: We analyze the coupling of model nonexcitable (non-neural) cells assuming that the cell membrane potential is the basic individual property. We obtain this potential on the basis of the inward and outward rectifying voltage-gated channels characteristic of cell membranes. We concentrate on the electrical coupling of a cell ensemble rather than on the biochemical and mechanical characteristics of the individual cells, obtain the map of single cell potentials using simple assumptions, and suggest procedures to collectively modify this spatial map. The response of the cell ensemble to an external perturbation and the consequences of cell isolation, heterogeneity, and ensemble size are also analyzed. The results suggest that simple coupling mechanisms can be significant for the biophysical chemistry of model biomolecular ensembles. In particular, the spatiotemporal map of single cell potentials should be relevant for the uptake and distribution of charged nanoparticles over model cell ensembles and the collective properties of droplet networks incorporating protein ion channels inserted in lipid bilayers.

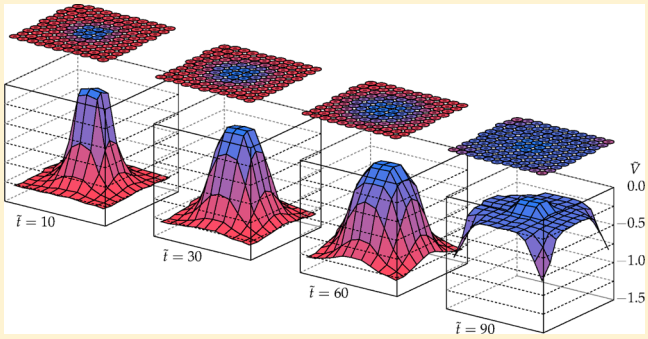

I. INTRODUCTION

The biophysical chemistry of a cell tissue involves different levels of description from the individual cellular machinery to the long-range intercellular coupling underlying multicellular organization. This fact is clearly shown, for example, in carcinogenesis models.[1−3] It has been argued[4] that this situation shows some similarities with the different chemical perspectives concerning the individual characteristics of single atoms and the collective properties of these atoms when organized in complex molecules. The coupling between the cells in a tissue involves not only biochemical pathways but also bioelectrical signals. Consider, for instance, the cell membrane potential, defined as the (negative) electrical potential difference between the cytoplasm and the extracellular environment when the electric current is zero. Depolarization processes characterized by abnormally low membrane potentials are characteristic of plastic (e.g., embryonic) cells[5−7] and epithelial wound healing,[8] while hyperpolarization tends to be associated with terminally differentiated cells.[5−7,9] However, since biochemical signals are essential to these biological processes, much emphasis is made on biochemical pathways rather than on bioelectric signals,[3] paying thus limited attention to the electrical transitions between the hyperpolarized and the depolarized cell states.[5,7,10] In particular, because the protein ion channels are expressed according to specific genes,[11−13] more attention is usually paid to channel genes than to the cell electrical state resulting from the action of multiple ion channels acting in concert.[14,15]

It has long been known that bioelectrical mechanisms can be relevant for subcellular organelles and the membrane cell (see refs 3, 15, and16, and references therein). Electromagnetic fields are also related with spatiotemporal patterns over tissues and can participate in the information exchange among cells (see refs 5 and 16−19, and references therein). These patterns are characterized by locally different electric potentials and ionic fluxes,[5] which are ultimately supported by the ion channels over the single cell membrane.[14] Voltage-gated channels are involved in the regulation of the cell electrical state because of their externally tunable electrical conductance.[14,20,21] Also, these channels can act as physical contacts (e.g., gap junctions[19,22−24]) between neighboring cells, allowing electrical coupling and communication. This type of coupling has not been addressed with detail in recent tissue models based on the theory of attractors (see, e.g., the reviews in refs 25 and 26). Previous Ising[27] and Potts[28] models tend to concentrate on local short-range interactions, describing the spatial correlations between the cells in a tissue,[29] and considering the normal to cancer tissue transition as a physical phase transition.[27,30] Alternatively, long-range diffusion-reaction,[4] diffusion-drift,[31−33] and cable[33] equations have described the spatiotemporal changes in model tissues using different numerical techniques (e.g., discretization). The electrophoretic transport through the intercellular junctions

Received: December 26, 2014
Revised: January 26, 2015
Published: January 26, 2015

DOI: 10.1021/jp512900x
J. Phys. Chem. B 2015, 119, 2968−2978

has also been described in morphogenesis and early left−right patterning theoretical studies,[34] as well as in the synchronization of coupled pancreatic cells.[35]

We propose to explore the electrical correlation between (highly simplified) model cells employing a formalism that has proved to be useful for the coupling of both biological cells[34,35] and locally interconnected nanoelectronic nodes in cellular neural networks.[36,37] Intercellular coupling can be achieved by different bioelectrical elements (e.g., by the protein channels forming the gap junctions between neighboring cells[22,24]) acting as effective conductances and capacitances. Disruption of the intercellular communication has been found in abnormal tissues (see refs 23 and 38−40, and references therein), but its detailed description requires the consideration of biochemical pathways. To emphasize the effects of the electrical coupling, we ignore these pathways and concentrate on simple but intuitive ideas that may constitute a complement to the fruitful biochemical description.

In addition to cell coupling, two loosely defined states are usually incorporated in tissue models; for instance, "normal" and "abnormal single cell states are invoked in tumor dynamics.[4] Because bistability is a crucial characteristic of excitable cells in neural networks,[41] it is of significance to explore its consequences for the case of non-excitable (non-neural) cells. We have recently addressed[42] the electrical coupling between the inward and outward-rectifying voltage-gated channels, which describe the single cell polarization state[14,20] and propose now to consider the case of a model cell ensemble.

We assume that the cell potential is a basic characteristic of the individual cells[3,5−7,18] and consider different scenarios for the electrical coupling of the whole cell ensemble, ignoring the biochemical and mechanical[43,44] characteristics of the individual cells. We obtain the spatial map of single cell potentials and suggest procedures to collectively modify this map, a question of significance for the distribution of charged nanoparticles over multicellular systems.[45−50] (Flow cytometry and fluorescence microscopy techniques have shown that the binding of charged nanoparticles to the cell surface is modulated by the membrane potential and the formation of charged nanoparticle−protein complexes.[50]) Biomolecular networks with microdroplets that mimic basic functions of multicellular systems can be formed with protein ion channels inserted in lipid bilayers.[51,52] Therefore, the physical chemistry approach developed here for the map of electric potentials can also be of significance for the modeling of these networks.

II. THEORETICAL METHODS

A. Membrane Potential Bistability. Voltage-gated channels show typically inward and outward rectifications, which permit the cell polarization state to be regulated by ionic conduction and other mechanisms.[14] The (negative) value of the membrane potential constitutes an experimental characteristic useful to describe this state: hyperpolarization is associated with a high (in absolute value) membrane potential while depolarization corresponds to a low (in absolute value) membrane potential; see Figure 1. For instance, anomalous inward-rectifying potassium channels with different biophysical characteristics are found in some tumor cell lines (compare Figure 6A with Figure 6B in ref 12), which show membrane potentials significantly different than those of normal cells (Figure 6C in ref 12).[6,7,10,18]

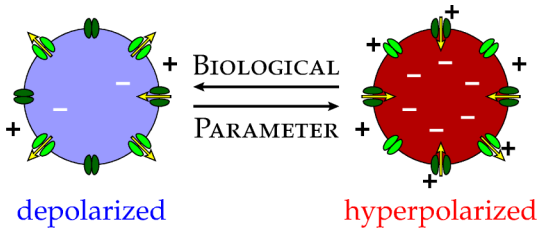

Figure 1. Model cell assumed here is a dynamical system showing transitions between the depolarized and hyperpolarized states, which are regulated by the inward and outward-rectifying ion channels.[42] The transitions are triggered by changes in the relevant biological parameters (e.g., the conductive characteristics of the ion channels and the ionic concentrations and the pH in the extracellular phase).

Although a multiplicity of ion channels distributed on the cell membrane contribute to the membrane potential, a highly idealized physical model showing bistability[42] can be constructed with only two physiologically relevant characteristics: the inward and outward electrical rectification shown in Figure 2a,b.[14,53−56] The potassium channels can conduct large inward currents at potentials more negative than the equilibrium potential E_{in} and low outward currents at potentials less negative than E_{in}.[14] This behavior can be approximately described by the simple current (I)-potential (V) phenomenological equation:

$$I = g(V - E_{in})P_{open}, \quad P_{open} = \frac{1}{1 + \exp[zF(V - V_{th})/RT]} \tag{1}$$

In eq 1, g is the maximum channel conductance, P_{open} is the open conductance probability, R, F, and T are the gas constant, the Faraday constant, and the temperature, respectively, and V_{th} is the threshold potential.[14,54,55] The steepness between the closed and open conductance states is described by the number of effective charges involved in channel gating, z.[14] Defining the dimensionless current $\tilde{I} = I/(gV_T)$, eq 1 can be rewritten as

$$\tilde{I} = (\tilde{V} - \tilde{E}_{in})P_{open}, \quad P_{open} = \frac{1}{1 + \exp[z(\tilde{V} - \tilde{V}_{th})]} \tag{2}$$

with the dimensionless potentials $\tilde{V} = V/V_T$, $\tilde{V}_{th} = V_{th}/V_T$, and $\tilde{E}_{in} = E_{in}/V_T$, where $V_T = RT/F = 27$ mV for $T = 310$ K. In the $\tilde{I} - \tilde{V}$ curve of Figure 2a, $\tilde{V} = 2$ corresponds to $V = 54$ mV and $\tilde{I} = 2$ is equivalent to $I = 54$ pA for a channel conductance $g = 1$ nS.[21,54] Figure 2b shows the curve corresponding to the outward rectifying channel, which results also from eq 2 by substituting E_{out} for E_{in} and reversing the sign of z.[14] The above channel characteristics, potentials, and currents are typical of some voltage-gated ion channels.[12−14,21,54−61]

The membrane potential $\tilde{V}_m = \tilde{V}(\tilde{I} = 0)$ is equal to the equilibrium Nernst potential $\tilde{E}_{in}$ for the potassium ion only if the contributions of the other (e.g., sodium and chloride) channels are ignored.[7,14] Note also the high conductance values obtained for hyperpolarization, $\tilde{V} < \tilde{E}_{in}$, contrary to the case of depolarization, $\tilde{V} > \tilde{E}_{in}$. The cell potential can be kept close to $\tilde{E}_{in}$ because of the small outward current that results from potentials more positive than $\tilde{E}_{in}$.[14] However, for potentials $\tilde{V}$ higher than the value giving the maximum in the $\tilde{I} - \tilde{V}$ curve of Figure 2a, the channel closes and enters a region of negative conductance, $d\tilde{I}/d\tilde{V} < 0$. The channel

DOI: 10.1021/jp512900x
J. Phys. Chem. B 2015, 119, 2968−2978

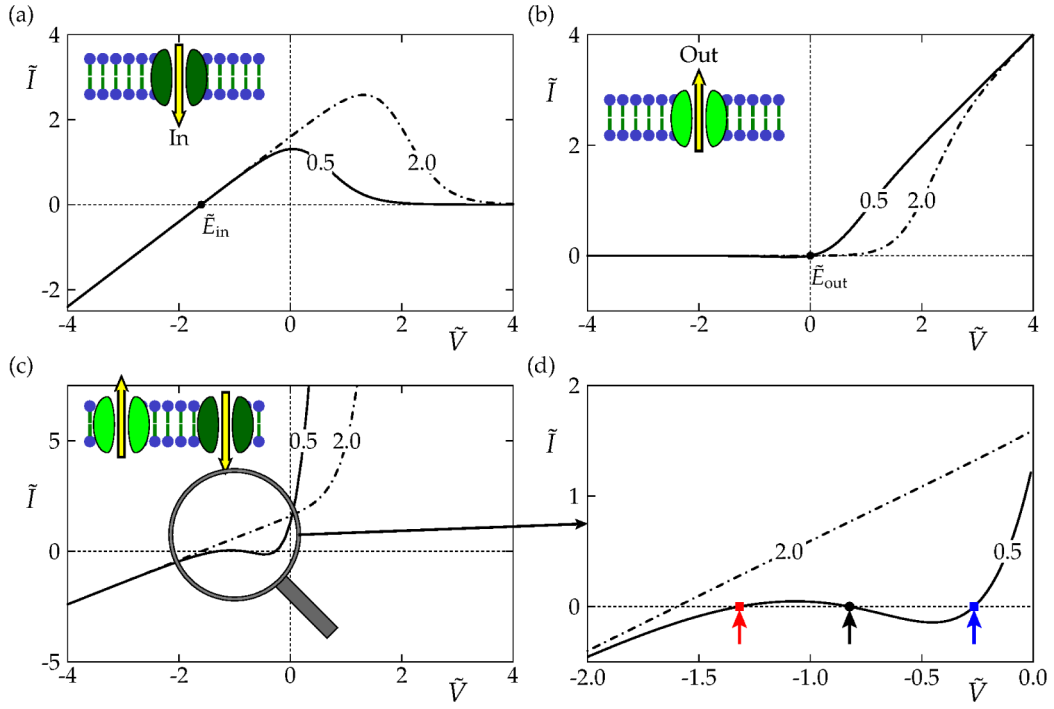

Figure 2. (a) $\tilde{I} - \tilde{V}$ curve of the inward-rectifying channel calculated from eq 2 with $z = 3$[14] and $\tilde{E}_{in} = E_{in}/V_T = -1.6$ (equivalent to $E_{in} = -41$ mV) for two values of the threshold potential, $\tilde{V}_{th} = 0.5$ and 2.0 (equivalent to $V_{th} = 13.5$ and 54 mV). (b) $\tilde{I} - \tilde{V}$ curve of the outward-rectifying channel with $z = -3$ and $\tilde{E}_{out} = 0$ in eq 2. (c) Current $\tilde{I} = \tilde{I}_{in} + \tilde{I}_{out}$ as a function of $\tilde{V}$ for N_{in} inward rectifying channels of maximum individual conductance g_{in} and potential $\tilde{E}_{in} = -1.6$ in parallel with N_{out} outward rectifying channels of conductance g_{out} and potential $\tilde{E}_{out} = 0$. The total conductance ratio is $G_{out}/G_{in} = N_{out}g_{out}/N_{in}g_{in} = 50$. (d) Bistability region of (c). The arrows correspond to the three solutions obtained for the membrane potential $\tilde{V}_m = \tilde{V}(\tilde{I} = 0)$ when $\tilde{V}_{th} = 0.5$. The central unstable potential at $\tilde{V}_m = -0.8$ (black, center) is surrounded by the stable hyperpolarized potential at $\tilde{V}_m = -1.3$ (red, left) and depolarized (blue, right) potential at $\tilde{V}_m = -0.3$. The insets of (a–c) schematically show the ion channels in the lipid bilayer forming the cell membrane.

closing may depolarize the potential $\tilde{V}$ to less negative values (Figure 2a), so that it is no longer possible to keep fixed the cell potential.[14,21,54] The above theoretical interpretation qualitatively describes the experimental trends observed in inward rectifying channels.[14,21,54,57] The properties of the external solutions (pH and ionic concentrations) can be incorporated in the equilibrium potential ($\tilde{E}_{in}$), while the channel characteristics are the threshold potential $\tilde{V}_{th}$, the effective charge z, and the conductance g.[14,54,61]

These voltage-gated ion channels constitute a simple, minimum model for membrane potential bistability (in practical cases, a multiplicity of channels may be involved[14]).). To show this question, Figure 2c gives the total current obtained by summing the individual contributions from the inward and outward rectifying channels in Figure 2a,b (the inset shows the region where the differential conductance is negative). The membrane potential is obtained by solving the equation of zero total current:

$$G_{in}(\tilde{V}_m - \tilde{E}_{in})\frac{1}{1 + \exp[z(\tilde{V}_m - \tilde{V}_{th,in})]} + G_{out}(\tilde{V}_m - \tilde{E}_{out}) \times \frac{1}{1 + \exp[-z(\tilde{V}_m - \tilde{V}_{th,out})]} = 0 \quad (3)$$

Three different membrane potentials $\tilde{V}_m$ can be obtained from eq 3 for certain values of the conductance and equilibrium potentials (Figure 2c,d). These potentials correspond to two stable (hyperpolarized and depolarized) values of $\tilde{V}_m$ and a central unstable value. Bistability has also been found in other models[60,62] and observed experimentally in hair cell membranes[63] as well as in individual skeletal and mouse lumbrical muscle cells.[60,64] Also, the slow voltage gating of lysenin channels inserted into lipid bilayer membranes has been described experimentally[65] and theoretically,[66] suggesting a biological memory unit based on the bistable pore response to external potentials. Finally, membrane potentials obtained for inward rectification conditions may also give two stable values because of the interplay between the rectifying channel and other elements in the electrical circuit.[67] Although the two channels of Figure 2 constitute only a crude model to describe the cell electrical state, it is remarkable that inward rectifying potassium channels are usually involved in the observed bistability phenomena,[60,63,64] showing the crucial physiological role of these voltage-gated channels.

Figure 3a shows the membrane potential $\tilde{V}_m$ obtained from eq 3 as a function of $\tilde{E}_{in}$ for different values of G_{out}/G_{in}, suggesting that the different values of the channel conductance ratio can give gradual transitions between the depolarized and hyperpolarized cell states as well as bistability phenomena. The shaded regions in the tridimensional space of Figure 3b correspond to fixed values of $\tilde{V}_{th}$ and show the zone where a bistability behavior similar to that of Figure 3a should be expected. This cell state space includes both bioelectrical characteristics at the cellular level (the channel conductance ratio G_{out}/G_{in} and the threshold potential $\tilde{V}_{th}$) and at multicellular level (the solution pH and ionic concentrations dictating the equilibrium potential $\tilde{E}_{in}$). As suggested previously by other authors,[6] cells with a similar physiological state may be located in particular regions of the

DOI: 10.1021/jp512900x
J. Phys. Chem. B 2015, 119, 2968–2978

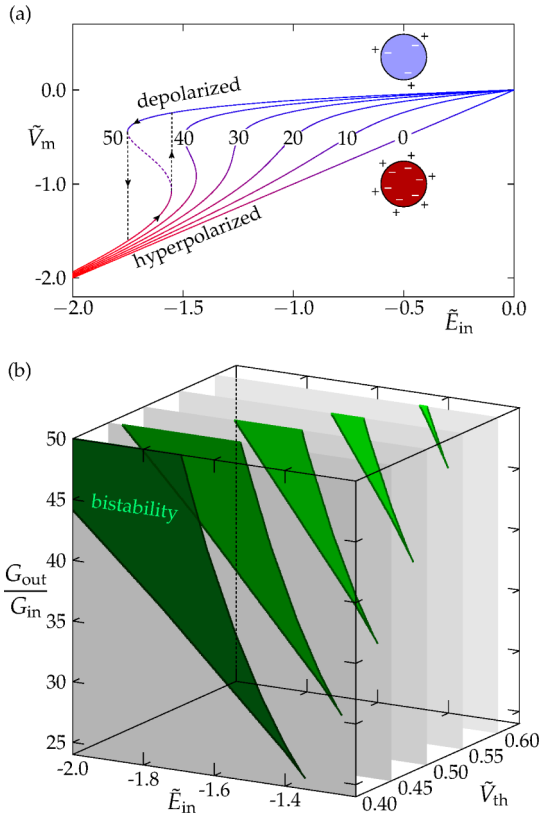

Figure 3. (a) Membrane potential $\tilde{V}_m$ vs $\tilde{E}_{in}$ curves parametric in G_{out}/G_{in} for $\tilde{V}_{th} = 0.5$ and $\tilde{E}_{out} = 0$. The arrows correspond to the transitions between the stable depolarized and hyperpolarized values while the dashed line corresponds to the unstable branch. (b) The shaded surfaces correspond to fixed values of $\tilde{V}_{th}$ and show those regions with a bistability behavior similar to that of (a). For the sake of clarity, the space has been truncated at the minimum values $\tilde{E}_{in} = -2.0$ and $\tilde{V}_{th} = 0.4$ and the maximum ratio $G_{out}/G_{in} = 50$.

above state space. Transitions between different cellular states can then be induced by modifying the values of the bioelectrical parameters in the axes[6] (e.g., by changing $\tilde{E}_{in}$ via the ionic concentrations or by changing the channel conductance because of the introduction of a blocking agent).

Figure 3a,b shows that two model cells with different ion channel characteristics (the ratio G_{out}/G_{in} here) may have significantly distinct membrane potentials. Although transitions between the normal and abnormal cell electrical states can result from the modification of the ion channels properties, changes in the ionic concentrations, which regulate the value of $\tilde{E}_{in}$,[14] may also result in modifications of the cell electrical state. In particular, Figure 3a shows that a gradual transition between the hyperpolarized and depolarized cell states can be obtained for those values of G_{out}/G_{in}, which are out of the bistable regions in Figure 3b.[42] Therefore, the cell electrical bistability is of significance only for a particular set of biological parameters (Figure 3b) in this model.

B. Cell Ensemble Model. Figures 2 and 3 have shown that a simple model with two voltage-gated channels can exhibit electrical bistability for certain values of the channel electrical characteristics and the external solution properties.[42] Bistability is not a necessary condition for our analysis, but it allows defining clearly the individual cell states in the spatial map of potentials that results from electrical coupling. We consider now an ensemble with N identical cells forming a small patch in a tissue model (the cases of anisotropic and heterogeneous coupling will be analyzed later). Intercellular communication is achieved here by an ionic conductance G in parallel with a capacitance C (Figure 4), as usual for simple

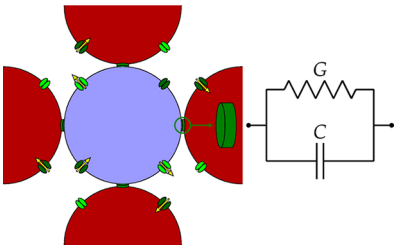

Figure 4. Central cell is connected to the four neighboring cells by effective coupling junctions described by identical conductances (G) and capacitances (C).

models of protein ion channels.[14] We emphasize however that this phenomenological approach does not invoke any particular biological structure (e.g., a specific protein gap junction with a nonlinear, potential dependent conductance[68]) for the effective coupling that should result because of cell–cell physical contact. The cell i ($i = 1, 2, ..., N$) is characterized by the time (t)-dependent electric potential $V_i(t)$, which may take any intermediate value between the depolarized and the hyperpolarized cell membrane potentials of Figure 2c. Local ionic currents may then flow through the junctions of adjacent cells to make equal their individual potentials, which allow changes in electric potential to progress from cell to cell over a cell ensemble.

Because we concentrate on electrical rather than chemical signals, we assume that the time evolution of the cell potentials is determined by the electrical currents $\tilde{I}_{in}$ and $\tilde{I}_{out}$.[63,67] Also, we take constant values for the equilibrium potentials $\tilde{E}_{in}$ and $\tilde{E}_{out}$, ignoring the ionic concentration changes that may occur for long experimental times.[59,60,64,68] This assumption should be approximately valid for the extracellular environment acting as a buffer that fixes the external ionic concentrations, but it is rather problematic for the intracellular ionic concentrations. However, the number of ions that must be transported across the membrane to set up typical potential differences is very small compared with the total number of ions in the cell, and then significant changes in the cell potential can result from small changes in the intracellular ionic concentrations.[24,59] Therefore, we will assume that the dynamics of the cell ensemble can be described by the individual cell potentials for short enough experimental times.[24,67]

According to the above assumptions, the potential $V_i(t)$ of cell i of Figure 4 should follow the time evolution equation

$$C_i \frac{dV_i}{dt} = -I_{in}(V_i) - I_{out}(V_i) + \sum_{j\ nn\ i} G_{ij}(V_j - V_i) + \sum_{j\ nn\ i} C_{ij}\left(\frac{dV_j}{dt} - \frac{dV_i}{dt}\right) + I_{ext} \quad (4)$$

where $C_i = C_0$ is the cell capacitance, $G_{ij} = G$ and $C_{ij} = C$ are the conductance and capacitance of the effective junction that couples cells i and j (Figure 4), $I_{in}(V_i)$ is given by eq 1 (note that $I_{out}(V_i)$ results also from eq 1 by substituting E_{out} for E_{in} and reversing the sign of z), and I_{ext} is an external

DOI: 10.1021/jp512900x
J. Phys. Chem. B 2015, 119, 2968–2978

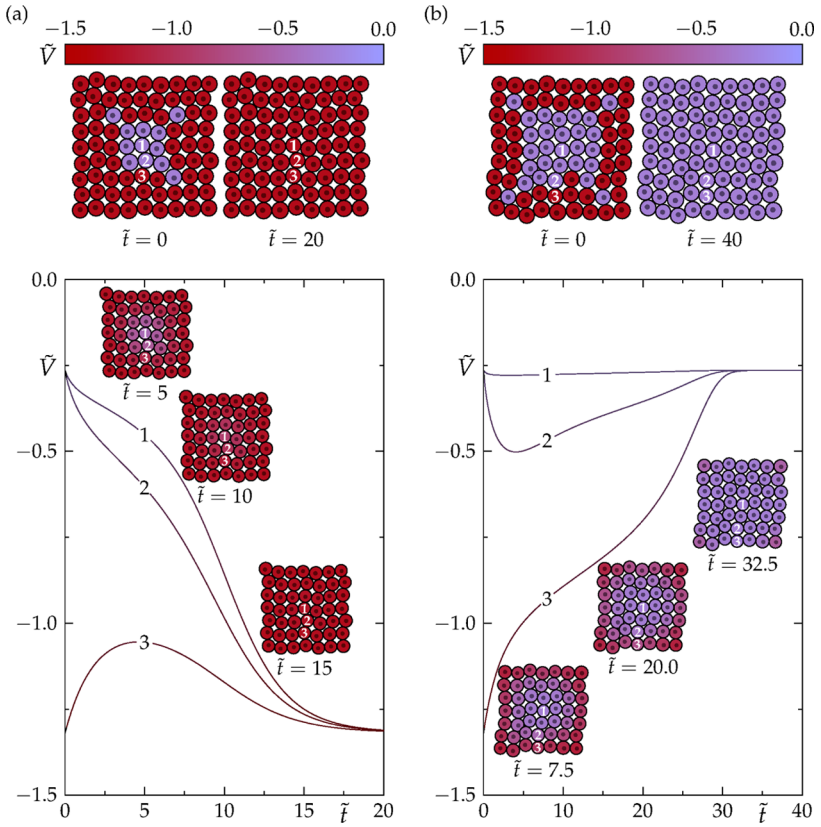

Figure 5. (a, b) Time evolution of the spatial map of cell potentials ($\tilde{V}$) for a model ensemble with 9 × 9 cells. The equilibrium potentials are $\tilde{E}_{in} = -1.6$ and $\tilde{E}_{out} = 0$, with $G_{out}/G_{in} = 50$ (see Figure 2c). Initially, most of the cells are in the hyperpolarized (red, dark) state except for a central region of depolarized (blue, light) cells. The top panel shows the initial and final maps of cell potentials. The bottom panel shows the time-dependent potentials of the three cells marked in the ensemble. The insets show an ensemble subset at three intermediate times. Normalization is possible only if the central region of initially depolarized cells is small (a), but the extension of the depolarized state to the rest of the cells could not be avoided in other cases (b). The system parameters are $G/G_{in} = 0.3$ (equivalent to 300 pS if $G_{in} = 1$ nS) and $C/C_0 = 0.3$ (equivalent to $C = 30$ pF for $C_0 = 100$ pF), with $I_{ext} = 0$.

perturbation (a current here). The summation index "j nn i" indicates restriction to the cell nearest neighbors ("nn") of Figure 4. Note that the extracellular environment provides a reference potential, which can be taken as zero, for the cell potentials V_i. Equation 4 shows that the changes in the individual cell potentials V_i are coupled to changes in the ionic currents $I_{in}(V_i)$ and $I_{out}(V_i)$ supported by the voltage-gated ion channels (eq 2). These regulation mechanisms acting at the cell level (see Figure 2c) are coupled at the multicellular level because of the junction network of Figure 4. In particular, anisotropic electrical couplings could contribute to symmetry breaking and spatiotemporal patterns.

All cells in the ensemble should be at exactly the same potential for arbitrarily large coupling conductances G. However, the fact is that G should take finite values in physiological junctions,[34,35] and thus, different cell potentials may exist over the cell ensemble, as we show later. We must note that other approaches similar to eq 4 have been previously used for describing the electrical coupling of locally interconnected nanostructures in neural networks,[36,37] providing the broad functionality and diversity of behaviors that should be expected for a model cell tissue.

Introducing the dimensionless variables used in eq 2 and Figure 2, eq 4 can be rewritten as

$$\dot{\tilde{V}}_i = -\frac{\tilde{V}_i - \tilde{E}_{in}}{1 + \exp[z(\tilde{V}_i - \tilde{V}_{th})]} - \frac{G_{out}}{G_{in}} \times \frac{\tilde{V}_i - \tilde{E}_{out}}{1 + \exp[-z(\tilde{V}_i - \tilde{V}_{th})]} + \frac{G}{G_{in}} \sum_{j \text{ nn } i} (\tilde{V}_j - \tilde{V}_i) + \frac{C}{C_0} \sum_{j \text{ nn } i} (\dot{\tilde{V}}_j - \dot{\tilde{V}}_i) + \frac{I_{ext}}{G_{in} V_T} \quad (5)$$

where the dot on the potentials denotes the derivative with respect to the dimensionless time $\tilde{t} = t/\tau$, $\tau = C_0/G_{in}$ ($\tilde{t} = 10$ is equivalent to $t = 1$ s for $C_0 = 100$ pF and $G_{in} = 1$ nS[67]). Although the capacitance term could provide an electrical coupling even for a conductance $G = 0$ in eq 5, the coupling conductance term should dominate over the capacitance term for typical values of G and C.[35,61,67] The potentials $\tilde{V}_i$ must be solved for $i = 1, 2, ..., N$ as a function of time to obtain the spatial map of cell potentials. We consider first the case of identical cells whose individual characteristics are those of Figure 2. Equation 5 can then be rewritten in matrix form and solved for $\tilde{V}_i$ as a function of time $\tilde{t}$ using periodic boundary conditions to minimize the effects of the finite number of cells in the ensemble. The numerical algorithm employed is described in the Supporting Information. We present the results graphically on a colored lattice to better show the multicellular state characterized by the spatial map of cell potentials.

DOI: 10.1021/jp512900x
J. Phys. Chem. B 2015, 119, 2968−2978

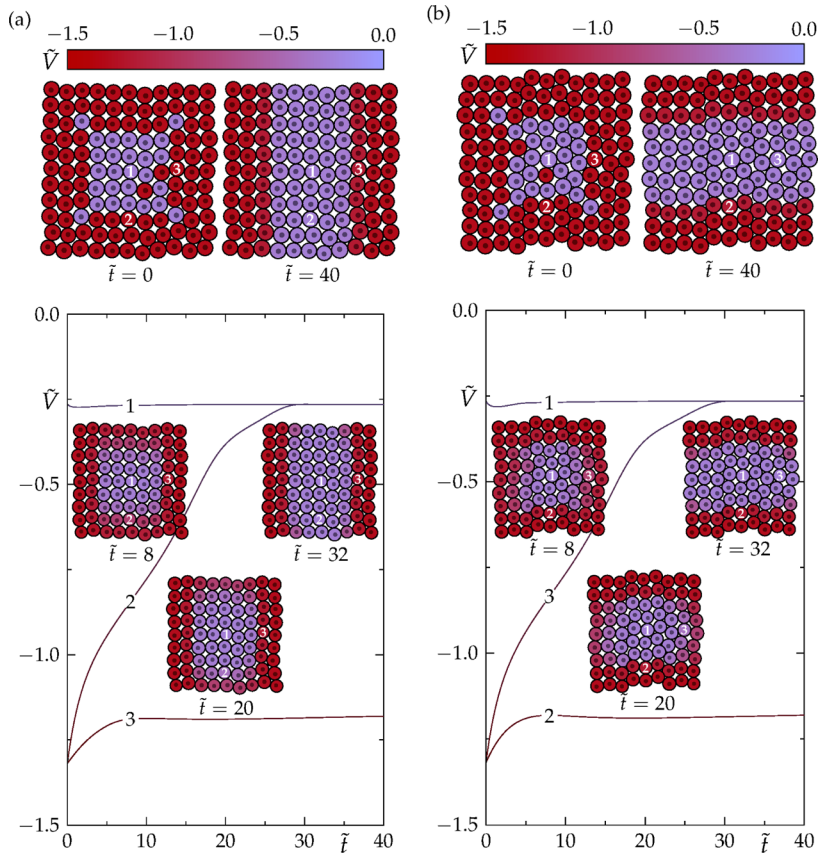

Figure 6. (a, b) The time evolution of the cell potentials for an ensemble of 11 × 11 cells with predefined vertical (a) and horizontal (b) depolarized patterns. As in Figure 5, G_{in}/G_{out} = 50, $\tilde{E}_{in}$ = −1.6, and $\tilde{E}_{out}$ = 0. Initially, most of the cells are in the hyperpolarized state except for the central region with cells in the depolarized state. The top Figure shows the initial and final states of the ensemble while the bottom Figure shows the time evolution of the potential for three marked cells. The insets correspond to an ensemble subset at three intermediate times. In (a), the system parameters are G/G_{in} = 0.3 and C/C_0 = 0.3 in the vertical direction (they are decreased to G/G_{in} = 0.05 and C/C_0 = 0.05 in the horizontal direction). In (b), the system parameters are G/G_{in} = 0.3 and C/C_0 = 0.3 in the horizontal direction (they are decreased to G/G_{in} = 0.05 and C/C_0 = 0.05 in the vertical direction). In both cases, I_{ext} = 0.

III. RESULTS AND DISCUSSION

Using eq 5, we have studied the time evolution of the cell potentials $\tilde{V}_i$ (i = 1, 2, ..., N) on the basis of the two stable states of Figure 2c. This evolution gives a spatiotemporal pattern for different case studies of bioelectrical significance: normalization of abnormal cells, spatial patterning following predefined directions, and system response to an external electrical perturbation. The effects of coupling conductance heterogeneity and ensemble size are considered later. In all cases, we have fixed the number of cells in the ensemble because we do not address the problem of tissue growth.

A. Normalization of Renegade Cells. Figure 5a shows the results obtained from eq 5 for the case of some depolarized (renegade) cells which are eventually hyperpolarized (normalized) because of the coupling to the neighboring cells. Obviously, this sort of "community effect" is allowed here by the cell electrical communication enforcing a local majority rule.[24] The top figure corresponds to the time evolution of the electrical potentials map, while the bottom figure shows the time-dependent potentials of three marked cells.

The above results show that the electrical coupling between neighboring cells can promote the normalization of a small number of abnormal, depolarized cells (Figure 5a), although the reverse case is also possible when the latter cells extend over a significant part of the model ensemble (Figure 5b). This normalization occurs because the dominant normal cells can change the individual electrical potential of the small group of abnormal cells, much as a physiological self-correction of a corrupted noisy image.[36] Clearly, the normalization process should be less effective for low coupling conductances, being not possible in the case of negligible coupling (G = 0 and C = 0 in Figure 4 and eq 5).

Although we have considered only electrical signals, the cell potentials regulate local ionic currents involved in the biochemical pathways that regulate the cell state.[19,22,34] It should also be mentioned that the permeability of protein gap junctions can be modulated externally[24] and that nonfunctional junctions causing defective intercellular communication can be found in abnormal tissues.[23,69]

B. Patterning of Predefined Spatial Directions. Spatial patterning is crucial in embryogenesis[5,6] and we explore now the question of ensemble patterning along predefined directions. Figure 6a shows the cell ensemble evolution when the horizontal coupling parameters are decreased with respect to those characteristic of the vertical coupling, thus, enhancing the patterning along the vertical direction. Figure 6b shows the opposite effect: if the vertical coupling conductance is decreased, horizontal patterning occurs in the ensemble. The vectorial nature of the electrical coupling, together with the anisotropy of the physical contacts between

DOI: 10.1021/jp512900x
J. Phys. Chem. B 2015, 119, 2968−2978

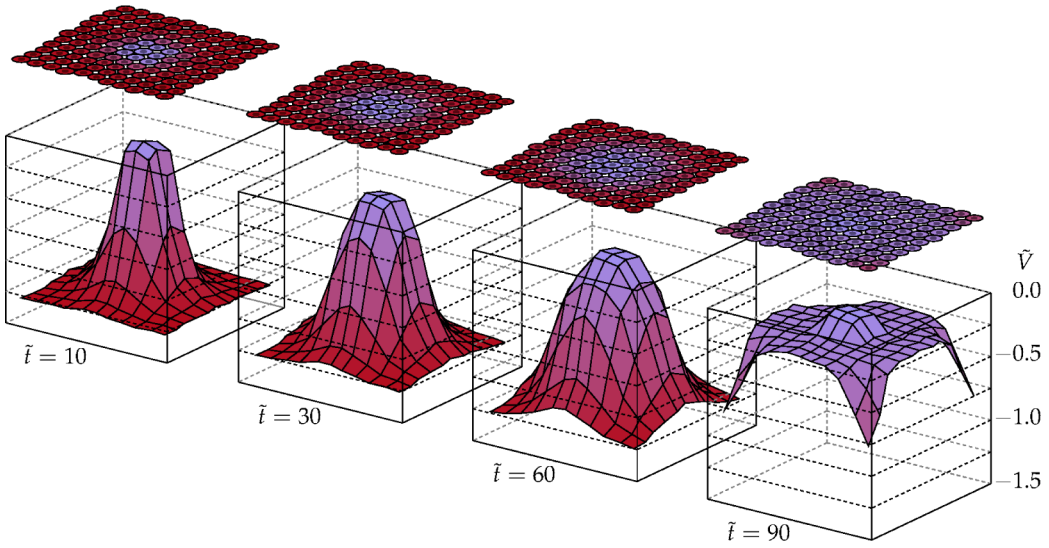

Figure 7. Time evolution of the cell potentials for a model ensemble with 11 × 11 cells following an external perturbation. The equilibrium potentials are $\tilde{E}_{in} = -1.6$ and $\tilde{E}_{out} = 0$, with $G_{in}/G_{out} = 50$ (Figure 5). Initially all the cells are in the hyperpolarized state. At a later stage, the constant current perturbation $I_{ext}/(G_{in}V_T) = 0.5$ is applied on the central region of the ensemble with 3 × 3 cells ($I_{ext}/(G_{in}V_T) = 0$ for the rest of the ensemble). Because of the cell coupling, the central pulse causes a bioelectrical wave which extends over the whole ensemble causing the depolarization. The system parameters are $G/G_{in} = 0.3$ and $C/C_0 = 0.3$.

cells, allow the progression of patterning, suggesting that an existing spatial asymmetry in the cell coupling parameters may act as an internal morphogenetic field.[5,6,19,34]

Exogenous and endogenous electric fields can redistribute small charged molecules over a multicellular ensemble because of the cell coupling.[70] Horizontal-vertical patterning could then result from the external action of biochemical and electrical agents (e.g., channel blockers) acting on the coupling junctions through electrically prepatterned spatial directions. Asymmetric patterns have indeed been observed in those cases where transport across the junctions does not occur equally in all directions.[19,71]

C. Bioelectrical Signal Propagation. A functional tissue is an open system, being subject to continuous biochemical, mechanical, and electrical perturbations. Figure 7 shows the time evolution of the model cell ensemble after being externally perturbed by an external injection of charge (the current I_{ext} in eq 4). The coupling between cells allows the propagation of the external perturbation to the whole ensemble, provoking the transition from a mostly hyperpolarized (normal) state to a mostly depolarized (abnormal) state. The opposite transition could be induced by reversing the initial state and the sign of the external perturbation.

Figure 7 shows that external perturbations can shift the individual state of the model cells over significant spatial regions. This result suggests that cell coupling could be used for reversing the electric potentials map by means of appropriate external agents, which may have implications for the uptake and transport of charged nanoparticles in tissues.[46−50] Note also that the external perturbation should progress predominantly along predefined spatial directions in the ensemble (see Figure 6) provided that an internal spatiotemporal field exists.

D. Cell Heterogeneity. Individual diversity should be accounted for in biological ensembles. In our case, the junctions may show significant heterogeneity because of local defects giving a number of defective cell−cell contacts. Note also that different electrical responses are experimentally obtained even for the same type of channels.[56] In the particular case of protein gap junctions, this heterogeneity could arise, for example, from small differences in the spatial orientation, geometry, and charge distribution of the individual ion channels. It has been shown that the membrane potential depends crucially on the fixed charge distributions in nanopores and membranes.[72]

Figure 8 revisits the normalization problem of Figure 5 for the case of (Gaussian) heterogeneous and homogeneous distributions of the coupling conductances. Although the normalization effect can be decreased in the presence of coupling conductance heterogeneity, it is still significant in Figure 8, suggesting that multicellular coupling can compensate for moderate biological diversity. Ordered heterogeneity[38] has been proposed as one of the basic characteristics of living systems because reliable collective properties should eventually emerge from individual diversity to ensure functional reliability.[75] Similar conclusions have been obtained for the synchronization of clusters of heterogeneous pancreatic β-cells by coupling gap junctions.[73,74] The results are also in qualitative agreement with previous Monte Carlo simulations concerning the effects of the individual variability on the average responses of biological (voltage-gated ion channels[75]) and artificial (nanowires[76]) networks of nanostructures showing a high heterogeneity. In these cases, individual differences can be tolerated because the coupling allows for a robust collective response.

E. Cell Ensemble Size. Figure 9 incorporates the effect of increasing the number of cells to $N = 10^4$. The conductance ratio has now been reduced to $G_{out}/G_{in} = 45$ with respect to the other figures to better show the normalization of the depolarized cells by the hyperpolarized ones. This small change in G_{out}/G_{in} shifts the unstable potential toward less negative values in Figure 2d, approaching the depolarized potential.[42] (Note that the cell potential tends to the hyperpolarized value for potentials between the unstable and the hyperpolarized values, while it goes to the depolarized value for potentials between the unstable and the depolarized

DOI: 10.1021/jp512900x
J. Phys. Chem. B 2015, 119, 2968−2978

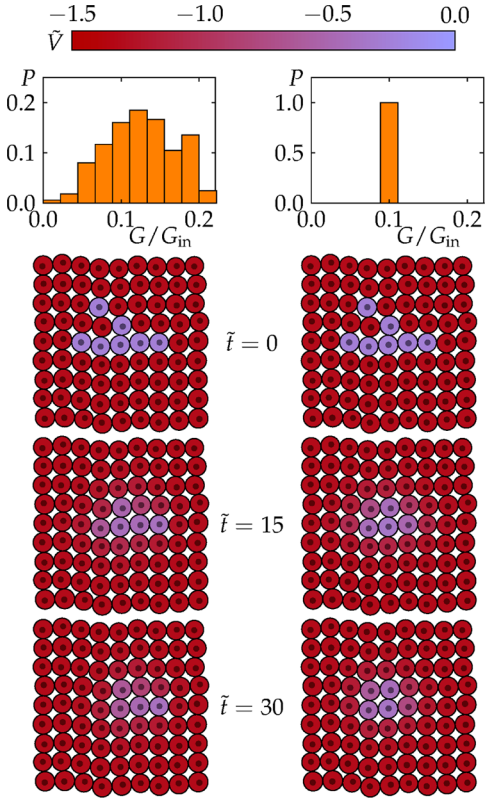

Figure 8. Time evolution of the cell potentials for the cases of a Gaussian statistical distribution of coupling conductances of probability P (left) and a uniform distribution (right). The system parameters are the same in the two cases, $\tilde{E}_{in} = -1.6$, $\tilde{E}_{out} = 0$, $G_{in}/G_{out} = 50$, $C/C_0 = 0.1$, and $I_{ext} = 0$.

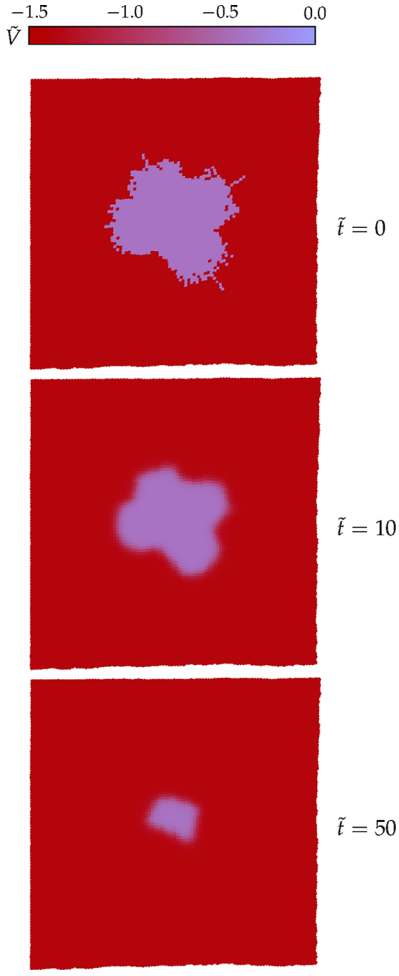

Figure 9. Time evolution of the cell potentials in an ensemble of $N = 100 \times 100$ cells with $\tilde{E}_{in} = -1.6$, $\tilde{E}_{out} = 0$ and $G_{in}/G_{out} = 45$. For sufficiently long times, normalization can reduce the extension of the central region of abnormal cells.

values; see Figure 2d.) As it could be expected, normalization takes a longer time in Figure 9 than in Figure 5 because of the significant increase in the ensemble size. However, the robust "community effect" supported by the large ensemble can eventually reduce the high number of abnormal cells initially present.

In summary, Figures 5−9 suggest that the spatial map of potentials can be externally modulated by exploiting the local electrical coupling between cells. In particular, the results show that coupling can promote cell normalization, provide internal mechanisms for patterning along predefined directions, and propagate an external bioelectrical signal. While the results are of qualitative value, we must note that the toy model used has serious limitations. Indeed, we have ignored the effects of ion pumps (passive ion transport makes a large contribution to the electrical potential across the plasma membrane in typical animal cells[24]) and assumed constant ionic concentrations (relatively short times are usually involved in electrophysiological experiments[58,67,68]). Also, additional ion channels and relevant biochemical signaling should be introduced for quantitative analysis of real biological problems.[16,59,60,64]

IV. CONCLUSIONS

We have used the electrical potential, a physiologically relevant characteristic,[5−7,18] to describe the collective state of a model multicellular ensemble in terms of the spatiotemporal map of individual cell potentials, which are regulated by ion channels. Because these protein aqueous pores are expressed by specific channel genes,[11−13] the genetic basis of the problem is only vaguely present in the theoretical approach. However, multicellular electric states may show complex feedback mechanisms that could not be readily deduced from considerations at the individual cell level only and it has been suggested that the physiological state (which is in part characterized by the map of electric potentials obtained here) may contribute to the regionalization of gene expression.[16]

For a particular set of biological parameters, bistability regions can be obtained in a multidimensional state space whose axis are defined by bioelectrical characteristics at the cellular and at the multicellular level,[6,42] consistent with the experimental fact that both properties are important.[1−3,18,77] Bistability is not crucial here, but it allows defining clearly the individual cell states (and then the spatial map of potentials) in Figures 5−9. We have then explored the electrical coupling via effective conductances and capacitances. These electrical elements may originate from specific protein ion channels, as is the case of intercellular gap junctions, or arise simply because of the close contact between cells. In this model, the phenomenological junctions that support the communication between cells can translate the electrical changes occurring at the single cell to the multicellular ensemble, allowing the

DOI: 10.1021/jp512900x
J. Phys. Chem. B 2015, 119, 2968−2978

normalization of small regions with abnormal cells and suggesting mechanisms for ensemble patterning. The normalization could not be possible when the number of abnormal cells is high or there exist partial cell isolation due to defective coupling (we cannot relate these phenomena to abnormal tissue growth because we have fixed the number of cells in the ensemble). Other results concern the perturbation of the system by an external electrical signal and the effects of cell number and heterogeneity.

The present approach ignores the biochemical pathways characteristic of real problems but provides intuitive physical insights using the basic building blocks of the multicellular electrical circuitry (individual cell ion channels and coupling junctions).[18,19,22,23] Obviously, the model is amenable to further extension, for example, by the incorporation of the reaction-diffusion processes characteristic of biochemical signaling[4,31,33] and the introduction of other biological elements[59,64] such as potential-dependent coupling conductances,[68] which can support multiple cell steady states. These extensions may suggest external procedures to collectively modify the electrical state of small regions within a model tissue. For instance, knowledge of the spatial map of potentials should be relevant for the modulation of the individual cell electrical states,[78] the blocking of specific ion channels by external agents,[55,79] the uptake and transport of charged nanoparticles over a multicellular system,[47−50] and the modeling of the collective properties of biomolecular droplet networks incorporating protein ion channels inserted in lipid bilayers.[51,52]

■ ASSOCIATED CONTENT

Supporting Information

The numerical algorithm used in the simulations is described. This material is available free of charge via the Internet at http://pubs.acs.org.

■ AUTHOR INFORMATION

Corresponding Authors

*Phone: +34 96 354 3926. E-mail: javier.cervera@uv.es.
*Phone: +34 96 354 3119. E-mail: smafe@uv.es.

Notes

The authors declare no competing financial interest.

■ ACKNOWLEDGMENTS

We acknowledge the financial support by the Generalitat Valenciana (Program of Excellence Prometeo/GV/0069), the Spanish Ministry of Economic Affairs and Competitiveness (MAT2012-32084), and FEDER. We thank Prof. Javier Garrido on occasion of his retirement for his continuous support.

■ REFERENCES

(1) Sonnenschein, C.; Soto, A. M. Theories of carcinogenesis: An emerging perspective. *Semin. Cancer Biol.* **2008**, *18*, 372−377.
(2) Baker, S. G.; Cappuccio, A.; Potter, J. D. Research on Early-Stage Carcinogenesis: Are we approaching paradigm instability? *J. Clin. Oncol.* **2010**, *28*, 3215−3218.
(3) Knox, S. S.; Funk, R. H. W. Oncology and biophysics: A need for integration. *J. Clin. Exp. Oncol.* **2014**, *S1*, DOI: 10.4172/2324-9110.S1-001.
(4) Cherubini, C.; Gizzi, A.; Bertolaso, M.; Tambone, V.; Filippi, S. A bistable field model of cancer dynamics. *Commun. Comput. Phys.* **2012**, *11*, 1−18.
(5) Levin, M. Large-scale biophysics: ion flows and regeneration. *Trends Cell Biol.* **2007**, *17*, 262−270.
(6) Levin, M. Molecular bioelectricity in developmental biology: New tools and recent discoveries. Control of cell behavior and pattern formation by transmembrane potential gradients. *Bioessays* **2012**, *34*, 205−217.
(7) Yang, M.; Brackenbury, W. J. Membrane potential and cancer progression. *Front. Physiol.* **2013**, *4*, 185.
(8) Chifflet, S.; Hernández, J. A.; Grasso, S. A possible role for membrane depolarization in epithelial wound healing. *Am. J. Physiol. Cell. Physiol.* **2005**, *288*, C1420−1430.
(9) Binggeli, R.; Weinstein, R. C. Membrane potentials and sodium channels: Hypotheses for growth regulation and cancer formation based on changes in sodium channels and gap junctions. *J. Theor. Biol.* **1986**, *123*, 377−401.
(10) Lobikin, M.; Chernet, B.; Lobo, D.; Levin, M. Resting potential, oncogene-induced tumorigenesis, and metastasis: the bioelectric basis of cancer *in vivo*. *Phys. Biol.* **2012**, *9*, 065002.
(11) Laforge, B.; Guez, D.; Martinez, M.; Kupie, J.-J. Modeling embryogenesis and cancer: an approach based on an equilibrium between the autostabilization of stochastic gene expression and the interdependence of cells for proliferation. *Prog. Biophys. Mol. Biol.* **2005**, *89*, 93−120.
(12) Bianchi, L.; Wible, B.; Arcangeli, A.; Tagliatatela, M.; Morra, F.; Castaido, P.; Crociani, O.; Rosati, B.; Faravelli, L.; Olivotto, M.; Wanke, E. Herg encodes a K+ current highly conserved in tumors of different histogenesis: A selective advantage for cancer cells? *Cancer Res.* **1998**, *58*, 815−822.
(13) Urrego, D.; Tomczak, A. P.; Zahed, F.; Stühmer, W.; Pardo, L. A. Potassium channels in cell cycle and cell proliferation. *Philos. Trans. R. Soc., B* **2014**, *369*, 20130094.
(14) Hille, B. *Ion Channels of Excitable Membranes*, 3rd ed.; Sinauer Associates: Sunderland, 1992.
(15) Mccaig, C. D.; Song, B.; Rajnicek, A. M. Electrical dimensions in cell science. *J. Cell Sci.* **2009**, *122*, 4267−4276.
(16) Adams, D. S.; Levin, M. Endogenous voltage gradients as mediators of cell−cell communication: strategies for investigating bioelectrical signals during pattern formation. *Cell Tissue Res.* **2013**, *352*, 95−122.
(17) Kline, D.; Robinson, K. R.; Nuccitelli, R. Ion currents and membrane domains in the cleaving xenopus egg. *J. Cell Biol.* **1983**, *97*, 1753−1761.
(18) Chernet B.; Levin, M. Endogenous voltage potentials and the microenvironment: Bioelectric signals that reveal, induce and normalize cancer. *J. Clin. Exp. Oncol.* **2013**, *S1*.
(19) Levin, M. Gap junctional communication in morphogenesis. *Prog. Biophys. Mol. Biol.* **2007**, *94*, 186−206.
(20) Fiske, J. L.; Fomin, V. P.; Brown, M. L.; Duncan, R. L.; Sikes, R. A. Voltage-sensitive ion channels and cancer. *Cancer Metastasis Rev.* **2006**, *25*, 493−500.
(21) Panama, B. K.; Lopatin, A. N. Differential polyamine sensitivity in inwardly rectifying Kir2 potassium channels. *J. Physiol.* **2006**, *571*, 287−302.
(22) Palacios-Prado, N.; Bukauskas, F. F. Modulation of metabolic communication through gap junction channels by transjunctional voltage; synergistic and antagonistic effects of gating and ionophoresis. *Biochim. Biophys. Acta* **2012**, *1818*, 1884−1894.
(23) Mesnil, M.; Crespin, S.; Avanzo, J.-L.; Zaidan-Dagli, M.-L. Defective gap junctional intercellular communication in the carcinogenic process. *Biochim. Biophys. Acta* **2005**, *1719*, 125−145.
(24) Alberts, B.; Johnson, A.; Lewis, J.; Raff, M.; Roberts, K.; Walter, P. *Molecular Biology of the Cell*, 4th ed.; Garland Science: New York, 2002.
(25) Huang, S.; Ernberg, I.; Kauffman, S. Cancer attractors: A systems view of tumors from a gene network dynamics and developmental perspective. *Semin. Cell Dev. Biol.* **2009**, *20*, 869−876.
(26) Bolouri, H. Network dynamics in the tumor microenvironment. *Semin. Cancer Biol.* **2015**, *30*, 52−59.

DOI: 10.1021/jp512900x
J. Phys. Chem. B 2015, 119, 2968−2978

(27) Torquato, S. Toward an Ising model of cancer and beyond. *Phys. Biol.* **2011**, *8*, 015017.
(28) Szabó, A.; Merk, R. M. H. Cellular Potts modeling of tumor growth, tumor invasion, and tumor evolution. *Front. Oncol.* **2013**, *3*, 87.
(29) Jiao, Y.; Berman, H.; Kiehl, T.-R.; Torquato, S. Spatial organization and correlations of cell nuclei in brain tumors. *PLoS One* **2011**, *6*, e27323.
(30) Davies, P. C. W.; Demetrius, L.; Tuszynsk, J. A. Cancer as a dynamical phase transition. *Theor. Biol. Med. Model.* **2011**, *8*, 30.
(31) Hassan, A. M.; El-Shenawee, M. Modeling biopotential signals and current densities of multiple breast cancerous cells. *IEEE Trans. Biomed. Eng.* **2010**, *57*, 2099−2106.
(32) Hassan, A. M.; El-Shenawee, M. Biopotential signals of breast cancer versus tumor types and proliferation stages. *Phys. Rev. E* **2012**, *85*, 021913.
(33) Léonetti, M.; Dubois-Violette, E.; Homblé, F. Pattern formation of stationary transcellular ionic currents in Fucus. *Proc. Natl. Acad. Sci. U.S.A.* **2004**, *101*, 10243−10248.
(34) Esser, A. T.; Smith, K. C.; Weaver, J. C.; Levin, M. Mathematical model of morphogen electrophoresis through gap junctions. *Dev. Dyn.* **2006**, *235*, 2144−2159.
(35) Sherman, A.; Rinzel, J. Model for synchronization of pancreatic beta-cells by gap junction coupling. *Biophys. J.* **1991**, *59*, 547−559.
(36) Karahaliloglu, K.; Balkir, S. Nanostructure array of coupled RTDs as cellular neural networks. *Int. J. Circ. Theor. Appl.* **2003**, *31*, 571−589.
(37) Bandyopadhyay, S.; Karahaliloglu, K.; Balkır, S.; Pramanik, S. Computational paradigm for nanoelectronics: self-assembled quantum dot cellular neural networks. *IEE Proc., Circuits Devices Syst.* **2005**, *152*, 85−92.
(38) Rubin, H. What keeps cells in tissues behaving normally in the face of myriad mutations? *Bioessays* **2006**, *28*, 515−524.
(39) Rubin, H. Rethinking "Cancer as a Dynamic Developmental Disorder" a quarter century later. *Cancer Res.* **2009**, *69*, 2171−2175.
(40) Capp, J.-P. Stochastic gene expression, disruption of tissue averaging effects and cancer as a disease of development. *BioEssays* **2005**, *27*, 1277−1285.
(41) Zhdanov, V. P. A neuron model including gene expression: bistability, long-term memory, etc. *Neural Process Lett.* **2014**, *39*, 285−296.
(42) Cervera, J.; Alcaraz, A.; Mafe, S. Membrane potential bistability in non-excitable cells as described by inward and outward voltage-gated ion channels. *J. Phys. Chem. B* **2014**, *118*, 12444−12450.
(43) Katira, P.; Bonnecaze, R. T.; Zaman, M. H. Modeling the mechanics of cancer: effect of changes in cellular and extra-cellular mechanical properties. *Front. Oncol.* **2013**, *3*, 145.
(44) Gonzalez-Rodriguez, D.; Guevorkian, K.; Douezan, S.; Brochard-Wyart, F. Soft matter models of developing tissues and tumors. *Science* **2012**, *338*, 910−917.
(45) Cheng, H.; Kastrup, C. J.; Ramanathan, R.; Siegwart, D. J.; Ma, M.; Bogatyrev, S. R.; Xu, Q.; Whitehead, K. A.; Langer, R.; Anderson, D. G. Nanoparticulate cellular patches for cell-mediated tumoritropic delivery. *ACS Nano* **2010**, *4*, 625−631.
(46) Poon, Z.; Chang, D.; Zhao, X.; Hammond, P. T. Layer-by-layer nanoparticles with a pH-sheddable layer for in vivo targeting of tumor hypoxia. *ACS Nano* **2011**, *5*, 4284−4292.
(47) Bonitatibus, P. J., Jr.; Torres, A. S.; Kandapallil, B.; Lee, B. D.; Goddard, G. D.; Colborn, R. E.; Marino, M. E. Preclinical assessment of a zwitterionic tantalum oxide nanoparticle X-ray contrast agent. *ACS Nano* **2012**, *6*, 6650−6658.
(48) Liu, X.; Chen, Y.; Li, H.; Huang, N.; Jin, Q.; Ren, K.; Ji, J. Enhanced retention and cellular uptake of nanoparticles in tumors by controlling their aggregation behavior. *ACS Nano* **2013**, *7*, 6244−6257.
(49) Arvizo, R. R.; Miranda, O. R.; Thompson, M. A.; Pabelick, C. M.; Bhattacharya, R.; Robertson, J. D.; Rotello, V. M.; Prakash, Y. S.; Mukherjee, P. Effect of nanoparticle surface charge at the plasma membrane and beyond. *Nano Lett.* **2010**, *10*, 2543−2548.
(50) Shin, E. H.; Li, Y.; Kumar, U.; Sureka, H. V.; Zhang, X.; Payne, C. K. Membrane potential mediates the cellular binding of nanoparticles. *Nanoscale* **2013**, *5*, 5879−5886.
(51) Holden, M. A.; Needham, D.; Bayley, H. Functional bionetworks from nanoliter water droplets. *J. Am. Chem. Soc.* **2007**, *129*, 8651−8655.
(52) Maglia, G.; Heron, A. J.; Hwang, W. L.; Holden, M. A.; Mikhailova, E.; Li, Q.; Cheley, S.; Bayley, H. Droplet networks with incorporated protein diodes show collective properties. *Nat. Nanotechnol.* **2009**, *4*, 437−440.
(53) Dahal, G. R.; Rawson, J.; Gassaway, B.; Kwok, B.; Tong, Y.; Ptácek, L. J.; Bates, E. An inwardly rectifying K^+ channel is required for patterning. *Development* **2012**, *139*, 3653−3664.
(54) Lu, Z. Mechanism of rectification in inward-rectifier K^+ channels. *Annu. Rev. Physiol.* **2004**, *66*, 103−129.
(55) Oliver, D.; Baukrowitz, T.; Fakler, B. Polyamines as gating molecules of inward-rectifier K1 channels. *Eur. J. Biochem.* **2000**, *267*, 5824−5829.
(56) Arcangeli, A.; Bianchi, L.; Becchetti, A.; Faravelli, L.; Coronnello, M.; Mini, E.; Olivotto, M.; Wanke, E. A novel inward-rectifying K^+ current with a cell-cycle dependence governs the resting potential of mammalian neuroblastoma cells. *J. Physiol.* **1995**, *489*, 455−471.
(57) Anumonwo, J. M. B.; Lopatin, A. N. Cardiac strong inward rectifier potassium channels. *J. Mol. Cell Cardiol.* **2010**, *48*, 45−54.
(58) Fologea, D.; Krueger, E.; Lee, R.; Naglak, M.; Mazur, Y.; Henry; Salamo, R. G. Controlled gating of lysenin pores. *Biophys. Chem.* **2010**, *146*, 25−29.
(59) van Heukelom, J. S. The role of the potassium inward rectifier in defining cell membrane potentials in low potassium media, analyzed by computer simulation. *Biophys. Chem.* **1994**, *50*, 345−360.
(60) van Mila, H.; van Heukelom, J. S.; Bier, M. A bistable membrane potential at low extracellular potassium concentration. *Biophys. Chem.* **2003**, *106*, 15−21.
(61) Cervera, J.; Mafe, S. Threshold diversity effects on the electric currents of voltage-gated ion channels. *Europhys. Lett.* **2013**, *102*, 68002.
(62) Léonetti, M. On biomembrane electrodiffusive models. *Eur. Phys. J. B* **1998**, *2*, 325−340.
(63) Jørgensen, F.; Kroese, A. B. A. Ion channel regulation of the dynamical instability of the resting membrane potential in saccular hair cells of the green frog (Rana esculenta). *Acta Physiol. Scand.* **2005**, *185*, 271−290.
(64) Gallahera, J.; Biera, M.; van Heukelom, J. S. First order phase transition and hysteresis in a cell's maintenance of the membrane potential: An essential role for the inward potassium rectifiers. *Biosystems* **2010**, *101*, 149−155.
(65) Fologea, D.; Krueger, E.; Mazur, Y. I.; Stith, C.; Okuyama, Y.; Henry, R.; Salamo, G. J. Bi-stability, hysteresis, and memory of voltage-gated lysenin channels. *Biochim. Biophys. Acta* **2011**, *1808*, 2933−2939.
(66) Krueger, E.; Al Faouria, R.; Fologea, D.; Henry, R.; Straub, D.; Salamo, G. A model for the hysteresis observed in gating of lysenin channels. *Biophys. Chem.* **2013**, *184*, 126−130.
(67) Wilson, J. R.; Clark, R. B.; Banderali, U.; Giles, W. R. Measurement of the membrane potential in small cells using patch clamp methods. *Channels* **2011**, *5*, 530−537.
(68) Baigent, S.; Stark, J.; Warner, A. Modelling the effect of gap junction nonlinearities in systems of coupled cells. *J. Theor. Biol.* **1997**, *186*, 223−239.
(69) Enomoto, T.; Sasaki, Y.; Shiba, Y.; Kanno, Y.; Yamasaki, H. Tumor promoters cause a rapid and reversible inhibition of the formation and maintenance of electrical cell coupling in culture. *Proc. Natl. Acad. Sci. U.S.A.* **1981**, *78*, 5628−5632.
(70) Cooper, M. S.; Miller, J. P.; Fraser, S. E. Electrophoretic repatterning of charged cytoplasmic molecules within tissues coupled

DOI: 10.1021/jp512900x
J. Phys. Chem. B 2015, 119, 2968−2978

by gap junctions by externally applied electric fields. *Dev. Biol.* **1989**, *132*, 179−188.
(71) Serras, F.; Fraser, S.; Chuong, C. M. Asymmetric patterns of gap junctional communication in developing chicken skin. *Development* **1993**, *119*, 85−96.
(72) Ramírez, P.; Mafe, S.; Manzanares, J. A.; Pellicer, J. Membrane potential of bipolar membranes. *J. Electroanal. Chem.* **1996**, *404*, 187−193.
(73) Smolen, P.; Rinzel, J.; Sherman, A. Why pancreatic islets burst but single β cells do not. The heterogeneity hypothesis. *Biophys. J.* **1993**, *64*, 1668−1680.
(74) Stamper, I. J.; Jackson, E.; Wang, X. Phase transitions in pancreatic islet cellular networks and implications for type-1 diabetes. *Phys. Rev. E* **2014**, *89*, 012719.
(75) Cervera, J.; Manzanares, J. A.; Mafe, S. The interplay between cooperativity and diversity in model threshold ensembles. *J. R. Soc. Interface* **2014**, *11*, 20140099.
(76) Cervera, J.; Claver, J. M.; Mafe, S. Individual variability and average reliability in parallel networks of heterogeneous biological and artificial nanostructures. *IEEE Trans. Nanotechnol.* **2013**, *12*, 1198−1205.
(77) Funk, R. H. W.; Thiede, C. Ion gradients and electric fields-an intrinsic part of biological processes. *J. Clin. Exp. Oncol.* **2014**, *S1*.
(78) Chernet, B. T.; Levin, M. Transmembrane voltage potential of somatic cells controls oncogene-mediated tumorigenesis at long-range. *Oncotarget* **2014**, *5*, 3287−3306.
(79) Arcangeli, A.; Crociani, O.; Lastraioli, E.; Masi, A.; Pillozzi, S.; Becchetti, A. Targeting ion channels in cancer: A novel frontier in antineoplastic therapy. *Curr. Med. Chem.* **2009**, *16*, 66−93.

DOI: 10.1021/jp512900x
J. Phys. Chem. B 2015, 119, 2968−2978